



ELSEVIER

Available online at www.sciencedirect.com

ScienceDirect

Journal of Magnetism and Magnetic Materials 320 (2008) e304–e307

www.elsevier.com/locate/jmmm

Synthesis and characterization of NiMn₂O₄ nanoparticles using gelatin as organic precursor

J.M.A. Almeida^{a,*}, C.T. Meneses^b, A.S. de Menezes^b, R.F. Jardim^c, J.M. Sasaki^a^aDepartamento de Física, Universidade Federal do Ceará, CP 6030, 60455-760 Fortaleza, CE, Brazil^bInstituto de Física “Gleb Wataghin”, Universidade Estadual de Campinas-UNICAMP, CP 6061, 13083-970 Campinas, SP, Brazil^cInstituto de Física, Universidade de São Paulo, CP 66318, 05315-970 São Paulo, SP, Brazil

Available online 21 February 2008

Abstract

Nanoparticles of NiMn₂O₄ were successfully obtained by mixing gelatin and inorganic salts NiCl₂·6H₂O and MnCl₂·4H₂O in aqueous solution. The mixture has been synthesized at different temperatures and resulted in NiMn₂O₄ nanoparticles with crystallites size in the range of 14–44 nm, as inferred from X-ray powder diffraction (XRPD) data. We have also observed that both the average crystallite size and the unit cell parameters increase with increasing synthesis temperature. Magnetic measurements confirmed the presence of a magnetic transition near 110 K.
© 2008 Published by Elsevier B.V.

PACS: 46.Df.+; 61.66.Hq; 61.66.Fn; 61.10.Nz; 68.03.Hj

Keywords: Nanoparticle; Gelatin; NiMn₂O₄; X-ray diffraction; Rietveld refinement

1. Introduction

The interest in the physics of nanoparticles has increased in the last years because of their different physical properties when compared to the corresponding bulk ones. In general, materials in bulk form with molecular formula AB₂O₄ present to have a normal spinel-type structure where atoms A (divalent cations) and B (trivalent cations) occupy tetrahedral and octahedral sites, respectively, and are distributed in the *fcc* lattice formed by the O²⁻ ions [1]. However, these materials may change their crystal structure for an inverse spinel or mixed spinel structure, a process that depends on the particle size. In the case of the inverse spinel structure, the A²⁺ ions occupy octahedral sites and the B³⁺ occupies both the tetrahedral and the octahedral ones. On the other hand, in the crystal structure known as the mixed spinel structure, atoms A and B occupy both octahedral and tetrahedral sites in materials with general formula (A_{1-x}B_x)[A_xB_{2-x}]O₄ [2]. Among several materials with the spinel structure, NiMn₂O₄, that crystallizes in a mixed spinel structure, is particularly of interest due to its physical properties as the temperature

dependence of the electrical resistance and catalytic activities [3,4]. Due to these and other features, several different methods have been used to synthesize NiMn₂O₄. However, in most of these methods high temperature and prolonged time of sintering are necessary, making them unsuitable for producing this spinel compound [3,5,6].

Recently, simple oxides as Cr₂O₃, NiO, and α-Fe₂O₃ were obtained by a chemical route where inorganic salts are mixed with gelatin and reacted at low temperature and for a short time [7–9]. The oxides prepared through this method exhibited crystallites with average size of 15 nm. Here, we report on a new and simple route for obtaining the binary oxide NiMn₂O₄. We have found that the material is comprised of nanoparticles with average size ranging from 14 to 44 nm. We also discuss the magnetic properties of these nanostructured spinel oxides [1].

2. Experimental

The samples were prepared from two different solutions: one with 1.04 g of gelatin (SARGEL) and 0.766 g of NiCl₂·6H₂O (SIGMA), which were dissolved in 10 mL of distilled water, and another one comprised of 2.1 g of

*Corresponding author. Tel.: +55 85 3366 9917; fax: +55 85 3366 9450.
E-mail address: julina@fisica.ufc.br (J.M.A. Almeida).

gelatin and 1.225 g of $\text{MnCl}_2 \cdot 4\text{H}_2\text{O}$ (MERCK 99%), which were dissolved in 10 mL of water. Both solutions were mixed and maintained under stirring at temperature of 40 °C. The final solution, with pH nearly 4, was cooled slowly and a gel was formed. The gel was dried at 80 °C during 5 days and the resulted material was a xerogel (biopolymer). This xerogel was heated up to different sintering temperatures 600, 700, 800, 900, and 1000 °C in a rate of 10 °C/min. The annealing time interval was typically of 6 h. The X-ray powder diffraction (XRPD) analysis was performed in a Rigaku X-ray diffractometer using Bragg–Brentano geometry in the continuous mode with speed of 0.5°/min. $\text{Cu K}\alpha$ radiation was used and the tube operated at 40 kV and 25 mA. The X-ray diffraction patterns were taken in the range of 17–91° in order to cover the most intense peaks of the NiMn_2O_4 phase. The phase identification analysis has been made with the help of the powder diffraction database of International Centre for Diffraction Data (ICDD). Rietveld refinement [10] procedures were made by using the DBWS 9807 code [11]. The pseudo-Voigt function has been used to fit the peak profiles of the identified crystalline phases. The full-width at half-maximum (FWHM) of the peaks has been used to estimate the crystallites size. Asymmetry coefficients, scale factors, and lattice parameters for each phase and the background polynomial parameters, were simultaneously refined. The calculation of the crystallites size for all powders has been performed by using the Scherrer's equation [12].

The FWHM parameter has been corrected by the instrumental broadening using LaB_6 powder standard, as described by Maia et al. [8]. The average microstrain (ϵ), a parameter extracted from the refinement, has been determined for all samples. This microstrain and crystallites size are convoluted in the integral breadth of the peak profile and both parameters can be analytically separated [13] and calculated by using the relationship:

$$\frac{\beta \cos \theta}{\lambda} = \frac{1}{D} + \frac{4 \times \epsilon \times \sin \theta}{\lambda} \quad (1)$$

The microstrain is given by the angular coefficient and the crystallite size by the linear coefficient in a plot of $\beta \cos \theta / \lambda$ versus $\sin \theta$.

Thermogravimetric analysis was performed in a Shimadzu Differential Thermal Analyzer. The measurements were performed in airflow, with a flow rate of 50 mL/min, and in the temperature range 25–1000 °C with a heating rate of 10 °C/min. Measurements of magnetization as function of the temperature were performed in SQUID magnetometer for two samples of NiMn_2O_4 which were synthesized at 1000 and 600 °C.

3. Results and discussions

3.1. Thermogravimetric analysis

In order to gain further information regarding the precursor material, thermogravimetric TG and differential

thermal analysis DTA were performed and the results are displayed in Fig. 1. The TG data indicate a pronounced mass loss close to 100 °C, corresponding to the elimination of water, and another one near 310 °C, attributed to the break out of the polymeric chains of the organic substances related to the gelatin addition. In this process, occurring up to 600 °C, the mass loss can be mainly associated with CO_2 and CO and the beginning of the NiMn_2O_4 formation.

3.2. X-ray diffraction

Fig. 2 displays the calculated intensity (Rietveld refinement) and the experimental XRPD patterns for all samples. The results indicate that samples have the mixed spinel structure and peaks belonging to NiO, which decrease in intensity with increasing sintering temperature (see Table 1). The presence of NiO in samples heat-treated below 850 °C has been also observed elsewhere [5]. This can be related to a small nonstoichiometry proportion of nickel chloride or due to a large ionic distribution of Mn mainly in the site 8a, as observed previously [14] in $(\text{NiFe}_2\text{O}_4)_{1-x} + (\text{NiMn}_2\text{O}_4)_x$ for $0.5 \leq x \leq 1.0$. The inset in Fig. 2 shows a systematic shift of the {333} plane to lower 2θ values with increasing sintering temperature, an indicative of the expansion of the unit cell volume of ~0.9%.

The average size of the crystallites was calculated by using the FWHM of the crystallographic families {022}, {113}, {224}, and {333} which were extracted from the Rietveld refinements. Fig. 3 exhibits a pronounced increase of the average crystallites size and microstrain of the crystallographic family {111} with increasing sintering temperature, verified also for others planes families. Such an increase in the microstrain is certainly related to the large surface effect, an effect much more pronounced when the crystallites size is largely reduced. Williamson–Hall [13] plots, used here to calculate the microstrain, showed a positive angular coefficient, indicating that all samples have a positive expansion in their structure along

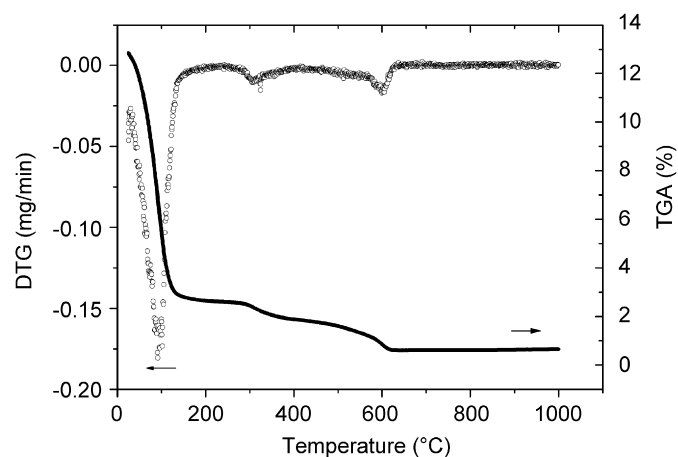


Fig. 1. TG and DTA analyses for the solution of the precursor material for the synthesis of the NiMn_2O_4 nanoparticles.

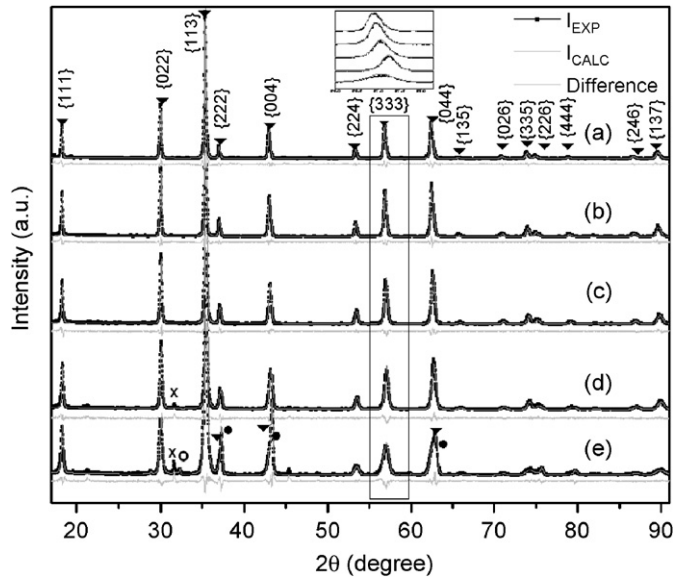


Fig. 2. X-ray powder diffraction patterns for samples heat-treated for 6 h: (●) NiO (cubic), (○) Mn₃O₄ (tetragonal), (▼) NiMn₂O₄ (cubic) and (×) peaks not identified. The patterns corresponding to samples heat-treated at (a) 1000 °C, (b) 900 °C, (c) 800 °C, (d) 700 °C, and (e) 600 °C.

Table 1
Crystallites size and concentration obtained by XRPD for samples synthesized for 6 h at different temperatures

Temperature (°C)	Practice size (nm)				Concentration (%)		
	Crystallographic families				NiMn ₂ O ₄	NiO	Mn ₃ O ₄
	{022}	{113}	{224}	{333}			
1000	44(2)	42(2)	33(1)	32(1)	99	1	–
900	41(2)	39(2)	32(1)	31(1)	97	3	–
800	35(1)	33(1)	27.2(8)	26.3(8)	97	3	–
700	31(1)	28.5(9)	23.3(6)	22.6(6)	94	6	–
600	22.9(6)	20.3(5)	14.9(3)	14.1(3)	87	12	1

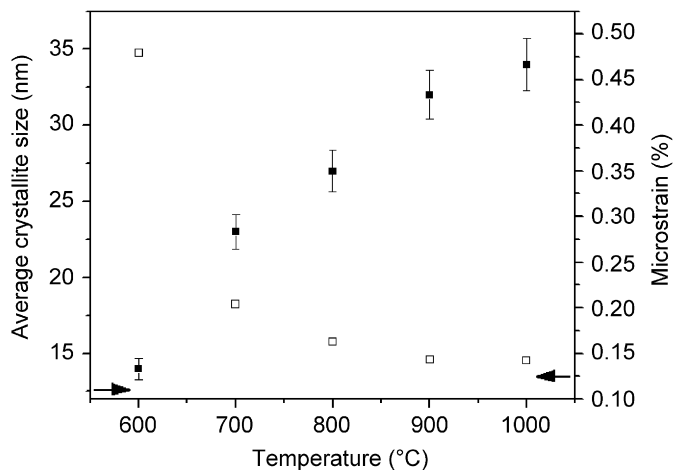


Fig. 3. Average crystallites size and microstrain as a function of the sintering temperature for the [1 1 1] direction.

the crystallographic direction [1 1 1], in agreement with the data displayed in the inset in Fig. 2.

3.3. Magnetic measurement

The temperature dependence of the magnetization, taken at 50 Oe and in the zero-field-cooling (ZFC) and field-cooling processes, is displayed in Fig. 4 for the samples sintered at 600 and 1000 °C. The curves show the onset of a ferrimagnetic transition at $T_C \sim 105$ and 110 K, respectively. These temperatures are slightly lower than that of $T_C = 145$ K observed in NiMn₂O₄ single crystal [1]. Such a decrease in T_C can be related to the reduction of the crystallite size of the samples or to the effect of oxygen vacancies, as discussed in Ref. [2].

From the temperature dependence of the magnetization above 200 K, we have extracted, by using the Curie–Weiss relationship, the magnetic moment per formula unit of the samples. For the sample sintered at 1000 °C, the estimated value is $\sim 7.1 \mu_B$ and for the sample sintered at 600 °C $\sim 6.9 \mu_B$. These values are in good agreement with that of $\sim 6.9 \mu_B$ calculated in single-crystal specimens [1]. They also found a Curie constant $C = 6.4$ emu K/mole for a sample prepared via the solid state reaction method and sintered at 1100 °C for 45 days. In any event, the small difference in the magnetic moment obtained for the sample

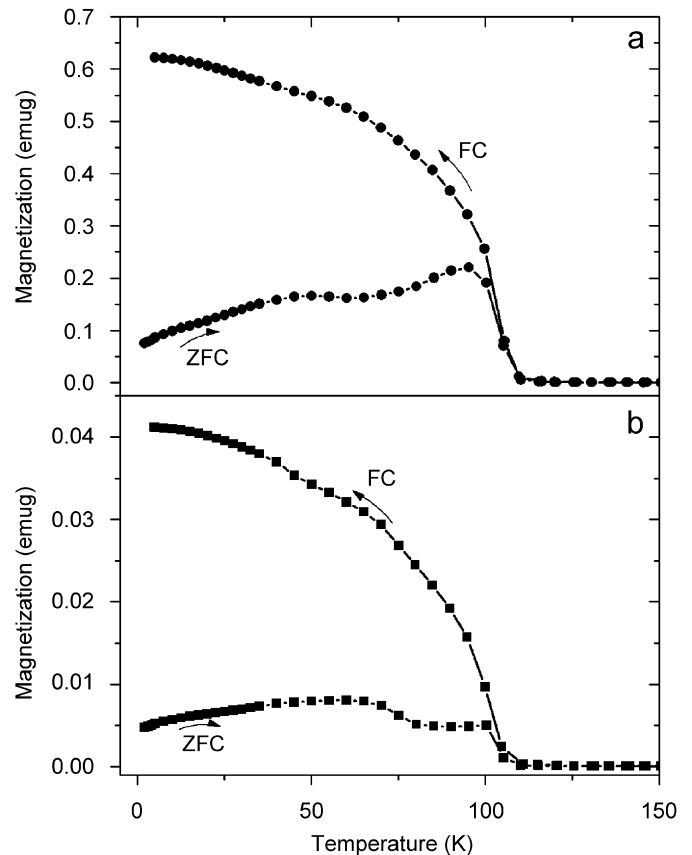


Fig. 4. ZFC and FC magnetization curves taken at $H = 50$ Oe for samples synthesized at (a) 600 °C and (b) 1000 °C.

heat-treated at 600 °C would be related to the small amount of NiO impurity phase, which decreases the magnitude of the magnetic moment due to the antiferromagnetic nature of NiO.

4. Conclusions

Nanoparticles of NiMn₂O₄, with average size between 14 and 44 nm, were produced by using gelatin as an organic precursor. Rietveld refinement analysis indicates that the nanoparticles crystallize in the mixed spinel structure and have a small amount of impurity phases. The samples show an increase in the crystallite size and a decrease in the microstrain with increasing sintering temperature. This can be used to control the size of the crystallites in this material. Magnetization measurements indicated a long-range ferrimagnetic ordering below 105 and 110 K, in samples sintered at 600 and 1000 °C. We finally argue that the simple and low cost method used here seems to be suitable to obtain NiMn₂O₄ nanoparticles at relatively low sintering temperatures.

Acknowledgments

The authors would like to thank the Brazilian agencies CNPq, CAPES, and FAPESP for the financial support and Gelita Brazil for supplying the gelatin used in this work.

References

- [1] S. Åsbrink, et al., *J. Phys. Chem. Solids* 58 (1997) 725.
- [2] P.N. Lisboa-Filho, et al., *Mater. Chem. Phys.* 85 (2004) 377.
- [3] R. Schmidt, A.W. Brinkman, *Int. J. Inorg. Mater.* 3 (2001) 1215.
- [4] D. Mehandjiev, et al., *Appl. Catal.* 206 (2001) 13.
- [5] Yi. Shen, et al., *J. Phys. Chem. Solids* 63 (2002) 947.
- [6] G. Ashcroft, et al., *J. Eur. Ceram. Soc.* 26 (2006) 901.
- [7] A.M.L. Medeiros, et al., *J. Metastable Nanocryst. Mater.* 20 (2004) 399.
- [8] A.O.G. Maia, et al., *J. Non-Cryst. Solids* 352 (2006) 3729.
- [9] A.S. de Menezes, et al., *J. Non-Cryst. Solids* 353 (2007) 1091.
- [10] H.M. Rietveld, *Acta Crystallogr.* 22 (1967) 151.
- [11] R.A. Young, et al., *Appl. Crystallogr.* 28 (1995) 366.
- [12] L.V. Azároff, *Elements of X-ray Crystallography*, McGraw-Hill, USA, 1968.
- [13] G.K. Williamsom, W.H. Hall, *Acta Metall.* 1 (1953) 22.
- [14] P.K. Baltzer, J.G. White, *J. Appl. Phys.* 29 (1958) 445.